Thin Solid Films 529 (2013) 111–114

Contents lists available at SciVerse ScienceDirect

Thin Solid Films

journal homepage: www.elsevier.com/locate/tsf

Influence of the GaN capping thickness on the strain and photoluminescence properties of InN/GaN quantum dots

Wen-Cheng Ke [a,*], Yue-Han Wu [b], Wei-Chung Houng [a], Chih-An Wei [a]

[a] Department of Mechanical Engineering, Yuan Ze University, Chung-Li 320, Taiwan, ROC
[b] Department of Materials Science and Engineering, National Chiao-Tung University, Hsin-Chu 300, Taiwan, ROC

ARTICLE INFO

Available online 29 May 2012

Keywords:
InN
Metal organic chemical vapor deposition
Capping layer
XRD
PL

ABSTRACT

InN quantum dots (QDs) were grown on 1 μm thick GaN/(0001) sapphire substrates by low pressure metal organic chemical vapor deposition. A single crystalline 10-nm thick GaN capping layer was achieved on the InN QDs by the flow-rate modulation epitaxy method at 650 °C. The (002) ω/2θ scans of the X-ray diffraction measurements show that the reduction of the lattice constant with a capping thickness indicate that the GaN capping process exerts a compressive strain on the InN QDs. The residual strain was reduced from 0.245% to −0.245% as the GaN cap thickness increases from 0 to 20 nm. In addition, the analysis of the photoluminescence peak energy estimated that the free electron concentration (i.e. density of indium (In) vacancy) decreased from 1.62×10^{18} cm^{-3} to 1.24×10^{18} cm^{-3}. The suggestion here is that the increase of the compressive strain on InN QDs due to the increased GaN capping layer thickness provides the high driving force for the interdiffusion of the In atom and gallium (Ga) atoms between the interface of InN QDs and the GaN capping layer. Thus, we believe that more Ga atoms can diffuse from the GaN capping layer and substitute the high density of In vacancy in the InN QDs, resulting in a decrease of the free electron concentration in the InN QDs with the increase in the GaN capping layer thickness.

1. Introduction

Revising the InN band gap energy to ~0.7 eV [1], has promised many additional applications of optoelectronic devices in the infrared range, including high efficiency solar cells and light emitting diodes. The InN quantum dots (QDs) are formed through self-assembly in the highly mismatched InN/GaN system (i.e., with a lattice mismatch of ~11%) by means of the "Stranski–Krastanov (SK: layer-plus-island)" growth mode [2]. The relaxation of the misfit strain was shown to be initiated by the formation of misfit dislocations (MDs) at the hetero-interface between InN and GaN [3–5]. The introduction of a low temperature GaN capping layer induces a rearrangement of the MDs at the InN/GaN capped interface [6]. In addition, the growth temperature of the GaN capping layer is limited, because of the low dissociation temperature of InN and the extremely high equilibrium vapor pressure of nitrogen. Generally speaking, low-temperature GaN film has poor crystal quality and a high defect density. These defects act as carrier trapping centers and limit the light-emitting and photo-voltaic efficiency of optoelectronic devices. Thus, it is essential that a systemic investigation of the strain distribution in InN QDs is carried out for high performance optoelectronic devices. Therefore, this paper presents a systematic study of the effect of GaN cap thickness on the structural and optical properties of InN/GaN QDs structures.

2. Experimental details

The InN/GaN QDs structures were grown on 1 μm thick GaN/(0001) sapphire substrates by metal organic chemical vapor deposition (MOCVD). The InN QDs were grown by pulsed mode (PM) method at a temperature of 650 °C to achieve higher density. The gas flow sequence for the PM method basically consists of four steps: 20 s trimethylindium (TMIn) + ammonia (NH_3) growth step, 20 s NH_3 source step with 10 s purge steps in between. During the growth step, the mole flow rates of TMIn and NH_3 are 1.53×10^{1} and 8.04×10^{5} μmole/min, respectively. The InN QDs layer is then covered with a thickness of 10 nm or 20 nm at 650 °C respectively, using the flow-rate modulation (FME) method. The mole flow rates of trimethylgallium (TMGa) and NH_3 are 2.21×10^{1} μmole/min and 1.79×10^{5} μmole/min, respectively for FME growth of GaN capping layer. The X-ray diffraction (XRD) was measured using a high resolution X-ray diffraction system—BRUKER D8 DISCOVER. This instrument is based around a two circle goniometer, enclosed in a radiation safety enclosure. The X-ray source is a 2.2 kW Cu anode long fine focus ceramic X-ray tube with Cu (Kα) radiation at 1.54 Å. The transmission electron microscopy (TEM) images of these samples were acquired by JEOL 2010F operated at 200 kV with a Gatan Orius 832 charge-coupled device. The specimen was prepared using a dual-beam focused ion beam facility with great

* Corresponding author. Tel.: +886 3 4638800; fax: +886 3 4558013.
E-mail address: wcke@saturn.yzu.edu.tw (W.-C. Ke).

0040-6090/$ – see front matter © 2012 Elsevier B.V. All rights reserved.
doi:10.1016/j.tsf.2012.05.040

care treatment. Because there were no obvious amorphous layers on the edge, we consider that there was little ion damage during our preparation. The photoluminescence (PL) measurements were performed using the 488-nm line of an argon-ion laser as the excitation source. The PL signals are dispersed by an ARC Pro 500 monochromator and were detected by a cooled InGaAs photodiode with a cutoff wavelength of 2.05 μm.

3. Results and discussion

The TEM image of the un-capped InN QDs is shown in Fig. 1(a). In Fig. 1(b), the high-resolution TEM (HRTEM) image shows the atomically sharp and flat 3 monolayers-thick InN wetting layer on top of the GaN buffer layer. The critical thickness for forming an InN QDs is about 0.86 nm. We believe that the InN QDs formation in this study was via the SK growth mode. However, the low dissociation temperature of InN and the extremely high equilibrium vapor pressure of nitrogen hindered the growth temperature of the GaN capping layer. Since the GaN capping layer is grown at a low temperature, the Ga adatom can't migrate to form a layer-by-layer growth, and instead leads to islanding. In this study, we attempted to grow the GaN capping layer by the FME technique (i.e. migration enhancement method). The precursor of TMGa and NH_3 were separately injected into the reactor in order to enhance the migration length of the Ga adatom [7]. The atomic layer epitaxy (ALE) method for GaN films grown at 550 °C by the MOCVD system has been reported to show good optical quality GaN films [8]. Fig. 1(c) shows the TEM image of the 10 nm thick GaN capping layer grown on the InN QDs by the FME technique. It has been found that a smooth GaN capping layer can be grown on the InN QDs. The enlarged HRTEM image of Fig. 1(d) was selected from the red-boxed area in Fig. 1(c). Obviously, the feature on the interface of the InN QDs and the GaN capping layer is differentiable. In order to confirm the single crystalline of GaN capping layer, we have examined the diffraction pattern and HRTEM micrographs. Fig. 2(a) illustrates a fast Fourier transform (FFT) of the image. The spots in the FFT image correspond to a diffraction pattern of the wurtzite structures of GaN-w and InN-w in the $[11\,2^{-}\,0]$ zone axis. It is worth noting that the sample does not contain any appreciable volume of other phases in the GaN or InN QDs regions. Fig. 2(b) shows a cross-sectional HRTEM micrograph viewed along the $[11\,2^{-}\,0]$ direction. The misfit dislocations appear at the interface between the InN QDs and the GaN capping layer. We also evaluated the GaN capping process on InN QDs. Fig. 1(a) shows that the height (h) and width (w) of the uncapped InN QDs are 19.6 nm and 103 nm, respectively, i.e. the aspect ratio (AR) h/w is about 1/5.3. After capping with a 10-nm thick GaN layer, the QDs width increases to 110 nm, while the dot height decreases to 17.8 nm (AR = 1/6.2). The change in morphology and the size changes of the QDs during capping have been widely reported for many material systems [9–11], and are usually explained as being the result of intermixing or the atomic exchange process. However, the change in aspect ratio of the InN QDs may be related to the strain in the InN QDs.

In order to study the strain level in the single-stacked InN QDs, we performed an X-ray diffraction measurement. Fig. 3(a) shows the (002) ω/2θ scans of the uncapped InN QDs and the InN QDs covered with various thicknesses of GaN capping layer. Combining Bragg's law with the expression for the inter-planar spacing in hexagonal structures, we find the lattice constant in the growth direction to be $c = l \times \lambda/(2 \sin \theta_B)$, for any allowed (00 l) reflection of X-rays of the wavelength λ. For this calculation, the lattice constant (c axis) of the GaN buffer layer is 5.185 Å, and the lattice constant (c axis) of the uncapped InN QDs is 5.717 Å. The values of the lattice constants for the case of stain-free InN are estimated to be in the range of c = 5.703 Å [12]. The larger lattice constant, c, is attributed to the biaxial compressive stress/strain in the basal plane, which is relieved to a large extend by plastic relaxation and results in a tensile strain along the c-axes. In contrast, the lattice constant is 5.689 Å for InN QDs covered by a 20-nm thick GaN capping layer. The reduction of the lattice constant with a capping thickness for a single-layer sample indicates that the GaN capping process exerts a compressive strain on

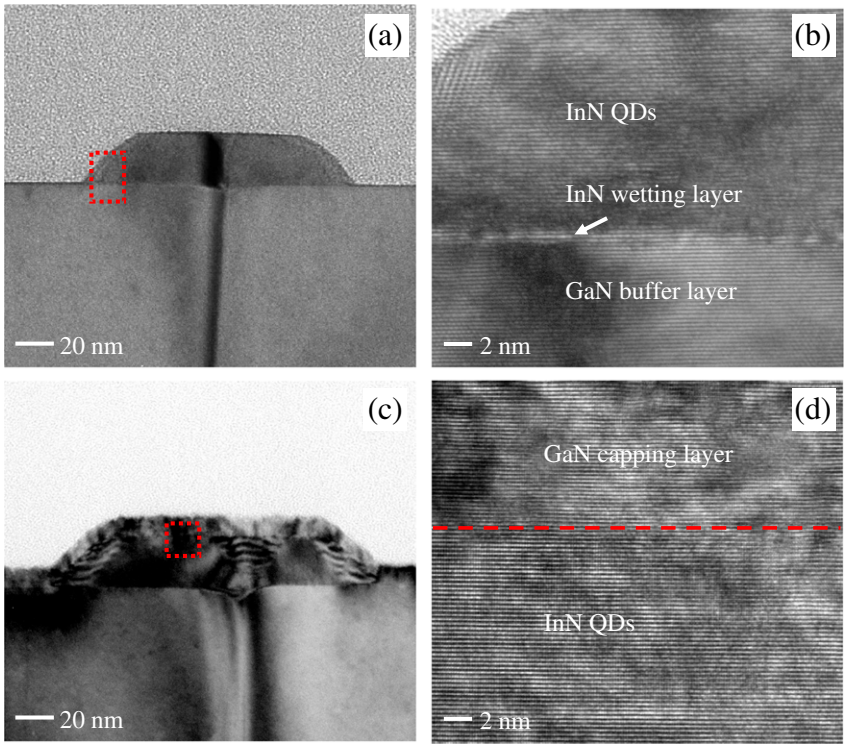

Fig. 1. TEM images of (a) un-capped InN QDs, and (b) the HRTEM image of un-capped InN QDs, and (c) InN QDs covered by a 10-nm thick GaN capping layer, and (d) the HRTEM image of InN QDs covered by a 10-nm thick GaN capping layer. Enlarged HRTEM images of (b) and (d) are from the red-boxed area in (a) and (c), respectively.

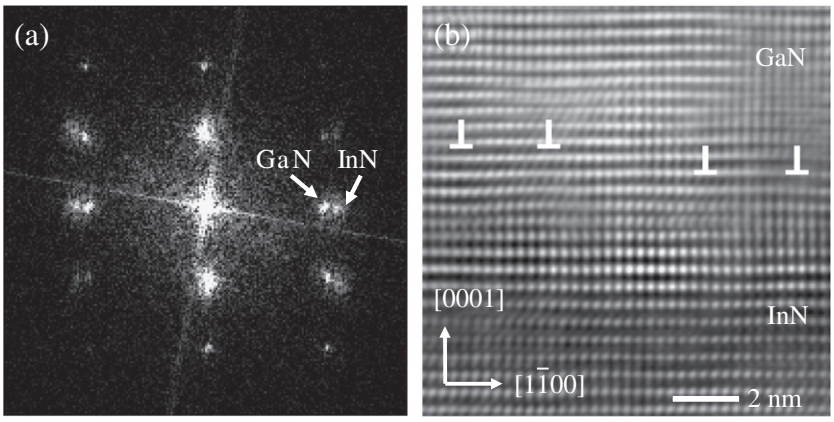

Fig. 2. (a) FFT image shows the characteristic wurtzite patterns for GaN and InN QDs. (b) HRTEM image of the GaN capping layer on the InN QDs interface viewed along [10]. The MDs marked by "⊥" are also shown.

the InN QDs. In addition, the residual strain relaxation in the InN QDs with different thickness of GaN capping layer were also studied. The strain (ε_{zz}) along the z axis was estimated from the relation,

$$\varepsilon_{zz} = \frac{C - C_0}{C_0} \times 100\% \quad (1)$$

where C denotes the lattice constant of the InN QDs and C_0 is a strain-free InN films. The residual strain is reduced from 0.245% to 0.07% as the GaN cap thickness increase from 0 to 10 nm. However, the residual strain of the InN QDs reduced to −0.245% for the 20-nm thick GaN capping layer.

Fig. 4 shows the 17K-PL spectra of the un-capped InN QDs, as well as the InN QDs covered with various GaN capping thicknesses. The Gaussian fitting of the PL spectrum for uncapped InN QDs shows a peak energy at 0.807 eV, with a full width at half maximum (FWHM) of 104 meV. In order to extract the InN QDs band gap energy (i.e. E_g), we consider the strain effect [13], confinement effect [14] and we calculate the electron Fermi energy (i.e. $\Delta E_F(n)$) [15] which is determined by the residual electron concentration in the InN QDs. The calculated results are summarized in Table 1. In InN/GaN system there is a large in-plane lattice mismatch, which is 98% of the initial compressive strain is relieved by the introduction of the misfit dislocation network [16,17]. The calculation of the strain effect on the InN/GaN QDs band gap (i.e. ΔE_{st}) is in the order of several meV, and is not the dominant effect on the PL peak energy. Since the height/width of uncapped InN QDs is 19.6/103 nm, the quantum confinement effect induced confinement energy (i.e. $\Delta E_{conf.}$) is about ~33.3 meV. Thus, the PL peak energy can be roughly estimated by $E_{PL} = E_g + \Delta E_{st} + \Delta E_{conf.} + \Delta E_F(n)$. The E_{PL} taken from the PL spectra, E_g, is assumed to be a constant value of 0.7 eV, $\Delta E_{conf.}$ which also can be calculated by the effective mass theory. The $\Delta E_F(n)$ is equal to $E_{PL} - E_g - \Delta E_{st} - \Delta E_{conf.}$. Finally, we can calculate the electron density in the InN/GaN QDs. The electron density is estimated to be 1.62×10^{18} cm^{-3} for uncapped InN QDs. The electron density decreased to 1.24×10^{18} cm^{-3} by increasing the GaN capping layer thickness to 20 nm. In addition, the PL FWHM can be decreased to 77 meV increasing the GaN capping thickness to 20 nm. The empirical relationship between the PL FWHM and the free-electron concentration provides a convenient formula to determine the free-electron concentration in InN films by PL, and was reported by Fu et al. [18]. There are many possible reasons that can influence the free carrier concentration in the

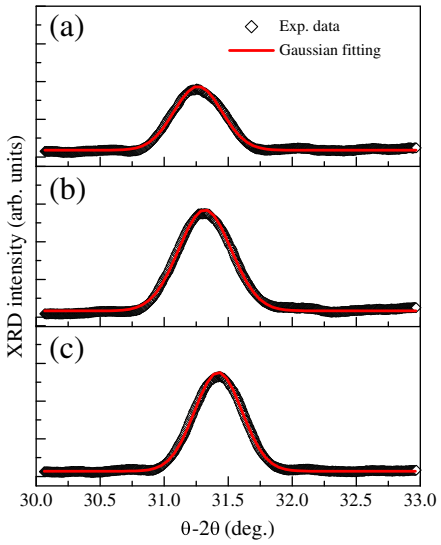

Fig. 3. The (002) XRD measurement of (a) un-capped InN QDs, InN QDs covered by (b) a 10-nm thick GaN capping layer, and (c) a 20-nm thick GaN capping layer. The Gaussian fitting curve of the XRD curve is shown by a red line.

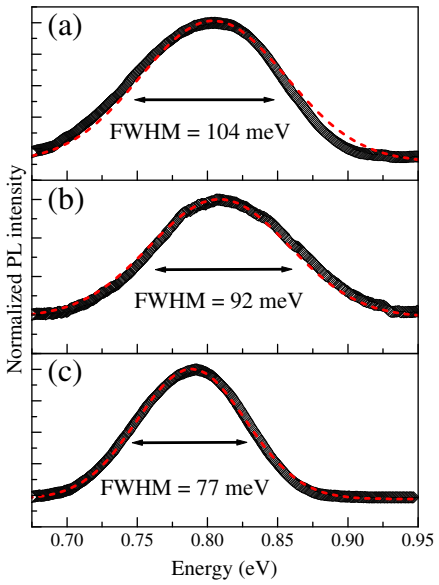

Fig. 4. The 17K PL spectra of (a) un-capped InN QDs, InN QDs covered by (b) a 10-nm thick GaN capping layer, and (c) a 20-nm thick GaN capping layer. The Gaussian fitting curve of the PL spectrum is shown by a red dashed line.

Table 1
The calculated results of the strain effect, confinement effect and the Fermi energy for the samples in this study.

	QDs height (nm)	E_{PL} (eV)	E_{st} (meV)	$\Delta E_{conf.}$ (meV)	$\Delta E_F(n)/n_e$ (meV)/(cm^{-3})
Uncapped	19.6	0.807	2.7	33.3	71 1.62×10^{18}
10 nm	17.8	0.804	0.8	39.9	63.3 1.36×10^{18}
20 nm	19.7	0.789	−2.8	32.6	59.2 1.24×10^{18}

uncapped InN QDs, such as surface states, oxidation [19] and/or surface near doping by oxygen. For capped InN/GaN QDs, the high atomic mobility and temperature instability of InN QDs may be caused by the intermixing. In addition, band bending due to the heterointerface and piezoelectric polarization charges in the InN/GaN QDs could play a role as well. Cimalla et al. [20] reported that the high surface electron concentration generated by the high surface density of states is due to the high ratio of surface area to volume of the QDs. It is well known that the thermal instability is due to the low InN dissociation temperature and high equilibrium N_2 vapor pressure over the InN, implying nitrogen desorption from the QDs [21]. Thus, we believe that GaN capping avoids InN decomposition and decreases the surface defect density.

In addition, the analysis of the PL peak energy does indicate a decrease of the free electron concentration in the InN QDs with the increasing GaN capping layer thickness. In this study, the aspect ratio of the uncapped InN QDs is about 1/5.3 and increases to 1/6.2 after being capped with a 10-nm thick GaN layer. The change in morphology of the QDs during capping for many material systems has been explained as being the result of intermixing or the atomic exchange process [9–11]. Some possible mechanisms including the group-III vacancy-related [22], impurity enhanced [23], or built-in field driven [24] mechanisms were proposed to be the driving force for the interdiffusion. Chyi et al. indicated that the high concentration of gallium vacancy was responsible for the interdiffusion of indium (In) and gallium (Ga) out of and within the InGaN/GaN quantum wells [25]. The analysis of the PL peak energy estimated that the electron concentration was about 1.62×10^{18} cm^{-3} for uncapped InN QDs. It also implied a high concentration of In vacancy in the uncapped InN QDs, since the In vacancy density was found to be correlated with free electron concentration of InN films [26]. The high concentration of In vacancy in the InN QDs indicated a high probability of interdiffusion between the interface of InN QDs and the GaN capping layer. In addition, the XRD results showed that the compressive strain increased with the increase in the thickness of the GaN capping layer. This increase in compressive strain enhances the driving force for the In and Ga atom interdiffusion between the interface of InN QDs and the GaN capping layer. We believe that the high density of In vacancy in the InN QDs can be substituted by more Ga atoms diffused from the GaN capping layer. Thus, the concentration of In vacancy in the InN QDs can be reduced by increasing the GaN capping thickness. The experimental results clearly indicate that the GaN capping layer grown by the FME method can be used for improving the optical properties of InN QDs. The present results are important for the multi-stack InN/GaN QDs structure.

4. Conclusions

In summary, we have investigated the structural and PL properties of InN/GaN QDs. A single crystalline 10-nm thick GaN layer was capped on the InN QDs by the flow-rate modulation epitaxy (FME) method. The XRD measurements showed that the reduction of the lattice constant with a capping thickness indicate that the GaN capping process exerts a compressive strain on the InN QDs. The increasing compressive strain enhanced the driving force for the In and Ga atom interdiffusion between the interface of InN QDs and the GaN capping layer. This suggests that more Ga atoms can be diffused into the InN QDs and substitute the inside In vacancy. Thus, the free electron concentration which relates to the In vacancy density can be reduced by increasing the thickness of the GaN capping layer. The GaN cap thickness is not only very important for the QDs strain but also for the emission properties of the InN QDs.

Acknowledgments

The authors gratefully acknowledge the financial support from the National Science Council of Taiwan, ROC under contract nos. NSC-98-2112-M155-001-MY3.

References

[1] J. Wu, W. Walukiewicz, K.M. Yu, J.W. Ager III, E.E. Haller, H. Lu, W.J. Schaff, Y. Saito, Y. Nanishi, Appl. Phys. Lett. 80 (2002) 3967.
[2] A. Yoshikawa, N. Hashimoto, N. Kikukawa, S.B. Che, Y. Ishitani, Appl. Phys. Lett. 86 (2005) 153115.
[3] S. Srinivasan, L. Geng, R. Liu, F.A. Ponce, Y. Narukawa, S. Tanaka, Appl. Phys. Lett. 83 (2003) 5187.
[4] Th. Kehagias, A. Delimitis, Ph. Komninou, E. Iliopoulos, E. Dimakis, A. Georgakilas, G. Nouet, Appl. Phys. Lett. 86 (2005) 151905.
[5] C.J. Lu, X.F. Duan, Hai Lu, W.J. Schaff, J. Mater. Res. 21 (2006) 1693.
[6] J.G. Lozano, A.M. Sánchez, R. García, D. González, M. Herrera, N.D. Browning, S. Ruffenach, O. Briot, Appl. Phys. Lett. 92 (2008) 231907.
[7] JunShuai Xue, JinCheng Zhang, YaoWei Hou, Hao Zhou, JinFeng Ahang, Yue Hao, Appl. Phys. Lett. 100 (2012) 013507.
[8] N.H. Karam, T. Parodos, P. Colter, D. McNulty, W. Rowland, J. Schetzina, N. El-Masry, Salah M. Bedair, Appl. Phys. Lett. 67 (1995) 94.
[9] Z. Zhong, J. Stangl, F. Schäffler, G. Bauer, Appl. Phys. Lett. 83 (2003) 3695.
[10] A. Hesse, J. Stangl, V. Holy, T. Roch, G. Bauer, O.G. Schmidt, U. Denker, B. Struth, Phys. Rev. B 66 (2002) 085321.
[11] J.G. Lozano, A.M. Sánchez, R. García, D. Gonzalez, O. Briot, S. Ruffenach, Appl. Phys. Lett. 88 (2006) 151913.
[12] I. Vurgaftman, J.R. Meyer, J. Appl. Phys. 94 (2003) 3675.
[13] C. Bayram, M. Razeghi, Appl. Phys. A 96 (2009) 403.
[14] W.C. Ke, C.P. Fu, C.Y. Chen, L. Lee, C.S. Ku, W.C. Chou, W.-H. Chang, M.C. Lee, W.K. Chen, W.J. Lin, Y.C. Cheng, Appl. Phys. Lett. 88 (2006) 191913.
[15] Wen-Hao Chang, Wen-Cheng Ke, Yu. Shu-Hung, Lin Lee, Ching-Yu Chen, Wen-Che Tsai, Hsuan Lin, Wu-Ching Chou, Ming-Chih Lee, Wei-Kuo Chen, J. Appl. Phys. 103 (2003) 104306.
[16] Wen-Che Tsai, Feng-Yi Lin, Wen-Cheng Ke, Lu. Shu-Kai, Shun-Jen Cheng, Wu-Ching Chou, Wei-Kuo Chen, Ming-Chih Lee, Wen-Hao Chang, Appl. Phys. Lett. 94 (2009) 063102.
[17] J.G. Lozano, A.M. Sánchez, R. García, D. González, M. Herrera, N.D. Browning, S. Ruffenach, O. Briot, Appl. Phys. Lett. 91 (2007) 071915.
[18] S.P. Fu, T.T. Chen, Y.F. Chen, Semicond. Sci. Technol. 21 (2006) 244.
[19] Tokuo Yodo, Yasunobu Kitayama, Kazunari Miyaki, Hiroaki Yona, Yoshiyuki Harada, Kathryn E. Prince, K. Scott, A. Butcher, J. Cryst. Growth 269 (2004) 145.
[20] V. Cimalla, V. Lebedev, F.M. Morales, R. Goldhahn, O. Ambacher, Appl. Phys. Lett. 89 (2006) 172109.
[21] W.L. Chen, R.L. Gunshor, J. Han, K. Higashimine, N. Otsuka, MRS Internet J. Nitride Semicond. Res. 2000 (2000) W3.30.
[22] W.M. Li, R.M. Cohen, D.S. Simons, P.H. Chi, Appl. Phys. Lett. 70 (1997) 3392.
[23] W.D. Laidig, J.W. Lee, P.K. Chiang, L.W. Simpson, S.M. Bedair, J. Appl. Phys. 54 (1983) 6382.
[24] B.I. Boltaks, Diffusion in Semiconductors, Academic, New York, 1963.
[25] C.-C. Chuo, C.-M. Lee, T.-E. Nee, J.-I. Chyi, Appl. Phys. Lett. 76 (2000) 3902.
[26] A. Laakso, J. Oila, A. Kemppinen, K. Saarinen, W. Egger, L. Liszkay, P. Sperr, H. Lu, W.J. Schaff, J. Cryst. Growth 269 (2004) 41.